Available online at www.sciencedirect.com
ScienceDirect
Ceramics International 36 (2010) 995–1009
CERAMICS INTERNATIONAL
www.elsevier.com/locate/ceramint

Synthesis of silicate glass/poly(L-lactide) composite scaffolds by freeze-extraction technique: Characterization and in vitro bioactivity evaluation

Abeer M. El-Kady [a,*], Ebtsam A. Saad [b], Bothaina M. Abd El-Hady [a], Mohmmad M. Farag [a]

[a] *Biomaterials Department, National Research Center, 33 El-Behooth St., Dokki, Giza, Egypt*
[b] *Chemistry Department, Ein Shams University, Cairo, Egypt*

Received 28 May 2008; received in revised form 3 September 2009; accepted 3 November 2009
Available online 29 November 2009

Abstract

The main objectives of the present study were to fabricate the silicate glass/poly(L-lactide) composite scaffolds for bone engineering applications, by using the freeze-extraction technique, and to evaluate the possibility for optimizing their degradation rate by changing their glass content. The scaffolds characterized by SEM-EDXA, FT-IR, TGA and XRD. Examination of the SEM microphotographs revealed that the pore size of the scaffolds decreased as the glass content increased. The neat polymer scaffold (PLA) had a highly interconnected porous structure with a maximum pore size of 200 μm. For the composite scaffold containing glass content up to 25 wt% (SP25) and up to 50 wt% (SP50), the maximum pore size was 40 μm and 20 μm respectively. The apparent porosity was 56.56%, 52.49% and 48.74% for PLA, SP25 and SP50, respectively. The results of the degradation study showed that the water absorption of the scaffolds decreased by increasing their glass content, It reached finally to 48.71%and 30.93% for SP25 and SP50, respectively. It revealed that also the weight loss of the scaffolds increased by increasing the glass content. The final weight loss was around 5.44%, 9.31% and 26.17% for the PLA, SP25 and SP50, respectively, indicating that it was possible to modulate the degradation rate of the scaffolds by varying their glass content. In addition, the pH measurement of incubation medium indicated that the glass could compensate the acidic degradation products of the polymer. In vitro bioactivity evaluation showed that the composite scaffolds were able to induce the formation of hydroxyapaptite layer on their surfaces, demonstrating their potential application in bone engineering.

Keywords: B. Composites; Bioactive glass; Scaffold; Bone engineering; Freeze-extraction

1. Introduction

In the tissue engineering approach, with the target of repairing large bone defects, a porous scaffold (artificial extracellular matrix) needed to accommodate cells and guide their growth and tissue regeneration in three dimensions [1]. In addition the scaffold must be biocompatible, biodegradable and bioactive to stimulate bone formation [2–5]. Aliphatic polyesters including poly(L-lactide) and poly (lactide-co-glycolide) were biocompatible and biodegradable and have been approved by the Food and Drug Administration (FDA) for certain human clinical applications [6]. However, they were not bioactive. On the other hand, silicate bioactive glasses in the system SiO_2–CaO–Na_2O–P_2O_5 have successfully been used in bone restoration and augmentation, middle-ear repair, vertebral replacement [7]. One of the most popular bioactive silicate-based glasses was the 45S5 Bioglass (45% SiO_2, 24.4% Na_2O, 24.5% CaO, and 6% P_2O_5 weight%) [8]. It had a strong stimulatory effect on bone cell function [9–13] and could regenerate bone tissue in vivo [14,15]. Therefore, the addition of bioactive glasses to the polyesters found to induce the bioactive property to them, and improve their biological activity, as well as their mechanical properties [16–25].

Highly porous bioactive glass/polymer composite scaffolds have been prepared by the freeze-drying technique [26–28]. During the freezing process, crystallization of the solvent took place and both polymer and bioactive glass particles expelled from the crystallization front, forming a polymer-glass-rich phase and a solvent-rich phase. After solvent sublimation, the polymer-glass rich phase forms a dense and continuous skeleton of the scaffold and the pores were fingerprints of the sublimated

* Corresponding author. Tel.: +202 33370933; fax: +202 33370931.
E-mail address: abeerelkady_2000@yahoo.co.uk (A.M. El-Kady).

0272-8842/$36.00.
doi:10.1016/j.ceramint.2009.11.012

solvent crystals. Although freeze-drying was widely used for the removal of the solvent crystals and generation of the porous scaffolds, it was time and energy consuming. In addition, using freeze-drying could lead to the formation of the surface skin. On the other hand, freeze-extraction was more suitable for the production of the porous scaffolds in large scale. Time and energy can be greatly saved. In the freeze-extraction method, the solvent removed by extraction with non-solvent. Therefore, the polymer would not dissolve because it is surrounded with non-solvent, hence it would be rigid enough to prevent pore collapse and formation of the surface skin [29]. In the presented study, the freeze-extraction instead of the freeze drying technique used to generate the porous structure of the glass/poly(L-lactide) composite scaffolds. The effect of glass content on the in vitro degradation of the composite scaffolds studied, to evaluated the possibility to optimize their degradation rate, by changing their glass content. The degradation process monitored by means of the measurement of the water uptake, weight loss and pH variation during the incubation period. The ability of the glass to compensate the acidic degradation products of the poly(L-lactide), as well as to provide a pH buffering action at its surface, also studied. Finally, the in vitro bioactivity evaluation carried out for the scaffolds, to ensure that they were able to induce the formation of hydroxyapatite layer on their surfaces.

2. Materials and methods

The poly L-lactide (M.Wt. 152,000) purchased from Fluka. Chloroform obtained from Acros (Acros Organics, Belgium).

2.1. Preparation of bioactive glass

45S5 bioactive glass prepared by weighing reagent grade amounts of raw materials. The reagents used in the preparation of glasses were SiO_2 (99.8%, quartz sand, Egypt), Na_2CO_3 (99.5%, ADWIA, Egypt), $CaCO_3$ (98.5%, BDH, UK) and $NH_4H_2PO_4$ (ARABLAB Company, UAE). The batch mixed well, melted in Rh–Pt crucible at about 1350 °C and homogenized for 3 h. The glass melt quenched in water and dried. The resultant glass frit ground in a ball mill to the grain size ranged from 63 μm to 50 μm. The glass given the code S for simplicity, the chemical composition of the glass listed in Table 1.

2.2. Preparation of silicate glass/poly(L-lactide) composite scaffolds

Two composite scaffolds prepared by the freeze-extraction technique. Details of the preparation method stated elsewhere [10–12,29]. Briefly, poly(L-lactide) dissolved in chloroform to form a polymer solution with a concentration of 12.5% (w/v). Bioactive glass powder added and the mixture stirred for 12 h to ensure the complete dissolution of the polymer and the formation of a homogenous solution. Then the solution froze at −80 °C. The vials containing the frozen glass/polymer solution immersed into an absolute ethanol solution at −80 °C to extract the chloroform. The ethanol changed three times a day for 2 days, then it removed by drying at the room temperature leading to the formation of the porous scaffolds. In addition to the composite scaffolds, a neat polymer scaffold prepared following the same method for comparison. The code of the scaffolds and their glass content are presented in Table 2. The glass content (25 wt%, 50 wt%) calculated according to Eq. (1):

$$\text{Glass content (wt\%)} = \left[\frac{\text{Wg}}{\text{Wg} + \text{Wp}}\right] \times 100 \quad (1)$$

where Wg was weight of the glass and Wp was weight of the polymer.

Table 1
Glass chemical composition (in wt%).

SiO_2	P_2O_5	CaO	Na_2O
45	6	24.5	24.5

Table 2
Scaffolds code and their glass content (wt%).

Scaffold code	Silicate glass content (wt%)
PLA	Neat polymer scaffold (containing no glass)
SP25	25 wt%
SP50	50 wt%

2.3. Characterization of the materials

The morphology and the porous structure of the scaffolds as well as their elemental composition analyzed with scanning electron microscopy coupled with energy-dispersive X-ray analysis (SEM/EDXA) (model JEOL JXA-840A, Electron Probe Microanalyzer) at 15 kV. The scaffolds cut with a razor blade and then coated with carbon or gold. The scanning electron microscope analysis carried out for each sample with different magnifications.

The infrared spectra of the prepared glass and scaffolds obtained using Fourier transformer infrared spectrophotometer (FT-IR) (model FT/IR-6100 type A) Spectra in wave number range of 400–4000 cm^{-1} recorded. Fine powders of the samples mixed with KBr powder in the ratio 1:100 and the mixtures subjected to a load of 10 tons/cm^2 to produce disc. Then, the infrared absorption spectra immediately measured after preparing the disc.

The phase analysis of samples examined by X-ray diffractometer (model BRUKER axs, D8ADVANCE) employing Ni-filtered and using Cu Kα irradiation at 40 kV and 25 mA. The XRD data collected over the 2θ range of 10–70° with a step size of 0.02°.

Table 3
Ionic concentration of simulated body fluid.

Description	Ionic concentration (mM)							
	Na^+	K^+	Mg^{2+}	Ca^{2+}	Cl^-	HCO^{3-}	HPO_4^{2-}	SO_4^{2-}
Plasma (human)	142.0	5.0	1.5	2.5	103.0	27.0	1.0	0.5
SBF	142.0	5.0	1.5	2.5	148.0	4.2	1.0	0.5

Thermogravimetric analyses (TGA) performed for the scaffolds using Computerized 7 series USA PerkinElmer thermal analysis system. Scans performed in an air atmosphere with a temperature range of 50–500 °C at a rate of 10 °C min^{-1}. The materials analyzed using aluminum oxide powder as a reference.

The bulk density and the apparent porosity of the scaffolds measured by the liquid displacement method as detailed elsewhere [30,31].

2.4. Degradation studies

In order to study the effect of the bioactive glass composition and its content on the degradation of the composite scaffolds, in vitro degradation tests carried out in phosphate buffer saline (PBS) (pH 7.4) at 37 °C. The degradation process monitored by means of the measurement of the water uptake, weight loss and pH variation in the PBS. Each scaffold placed into a vessel containing 50 mL of SBF and incubated for periods up to 30 days. At predetermined time periods, the samples removed from solution, and weighed wet after surface wiping, with an electronic balance to obtain the corresponding wet weight (W_{wet}). The dried weight (W_{dry}) of the samples is measured after drying the wet samples at 60 °C for 24 h in an oven and further at room temperature for 48 h in a vacuum chamber. The water-binding capacity (WA%) is calculated according to Eq. (4):

$$WA\% = \left[\frac{W_{wet} - W_{dry}}{W_{dry}}\right] \times 100 \quad (4)$$

The scaffold degradation determined as the percentage of the weight loss (WL%) and it obtained from the weight difference between the initial and the dried sample and

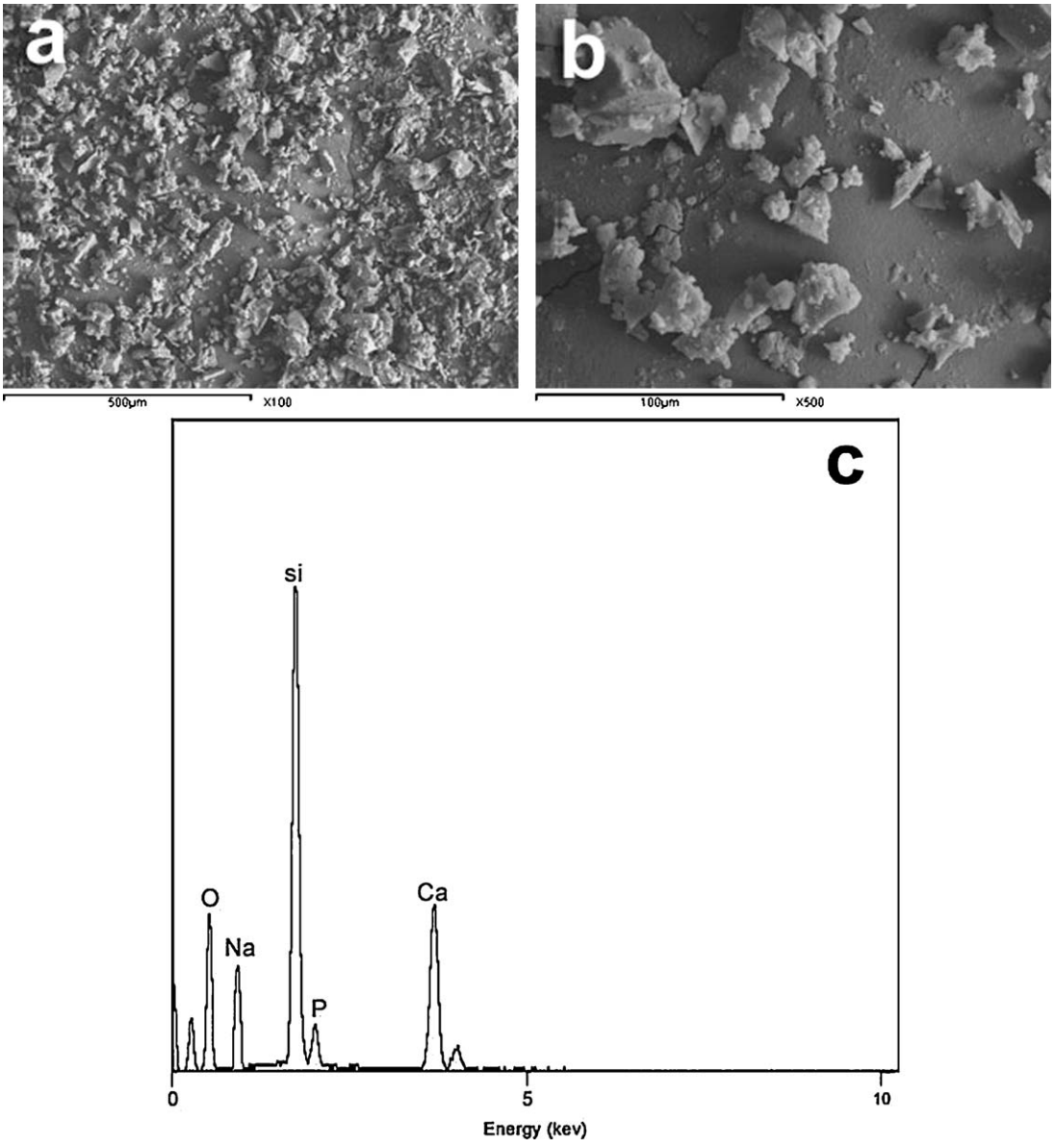

Fig. 1. SEM micrographs (a and b) and (c) EDX analysis of silicate glass (S).

calculated according to Eq. (5):

$$\mathrm{WL}\% = \left[\frac{W_{\mathrm{initial}} - W_{\mathrm{dry}}}{W_{\mathrm{initial}}}\right] \times 100 \quad (5)$$

2.5. In vitro bioactivity evaluation

The in vitro bioactivity of the scaffolds determined by soaking them in simulated body fluids (SBF) at 37 °C for various period of time. The SBF had an ion concentration nearly equal to that of the human blood plasma (Table 3). The SBF prepared by dissolving reagent-grade NaCl, $NaHCO_3$, KCl, $K_2HPO_4{\cdot}3H_2O$, $MgCl_2{\cdot}6H_2O$, $CaCl_2$, and $NaSO_4$ in deionized water. The solution buffered to pH 7.4 with Tris-(hydroxymethyl)aminomethane $(CH_2OH)_3CNH_3$) and hydrochloric acid [32]. The samples removed from the SBF, rinsed gently with absolute ethanol and then with deionized water, and left to dry. The formation of hydroxyapatite layer on the surface of the scaffolds verified by using scanning electron microscopy coupled with energy-dispersive X-ray analysis (SEM/EDXA)(-JEOL JXA-840A, Electron probe micro-analyzer) and thin-film X-ray analysis (TF-XRD) (Panalytical, X Pert Pro), employing Ni-filtered Cu Kα irradiation at 45 kV and 40 mA.

2.6. Statistic analysis

All data expressed by means of ±standard deviation (SD) for $n = 5$ and analyzed using standard analysis of Student's t-test. The level of significance is set at $p < 0.05$.

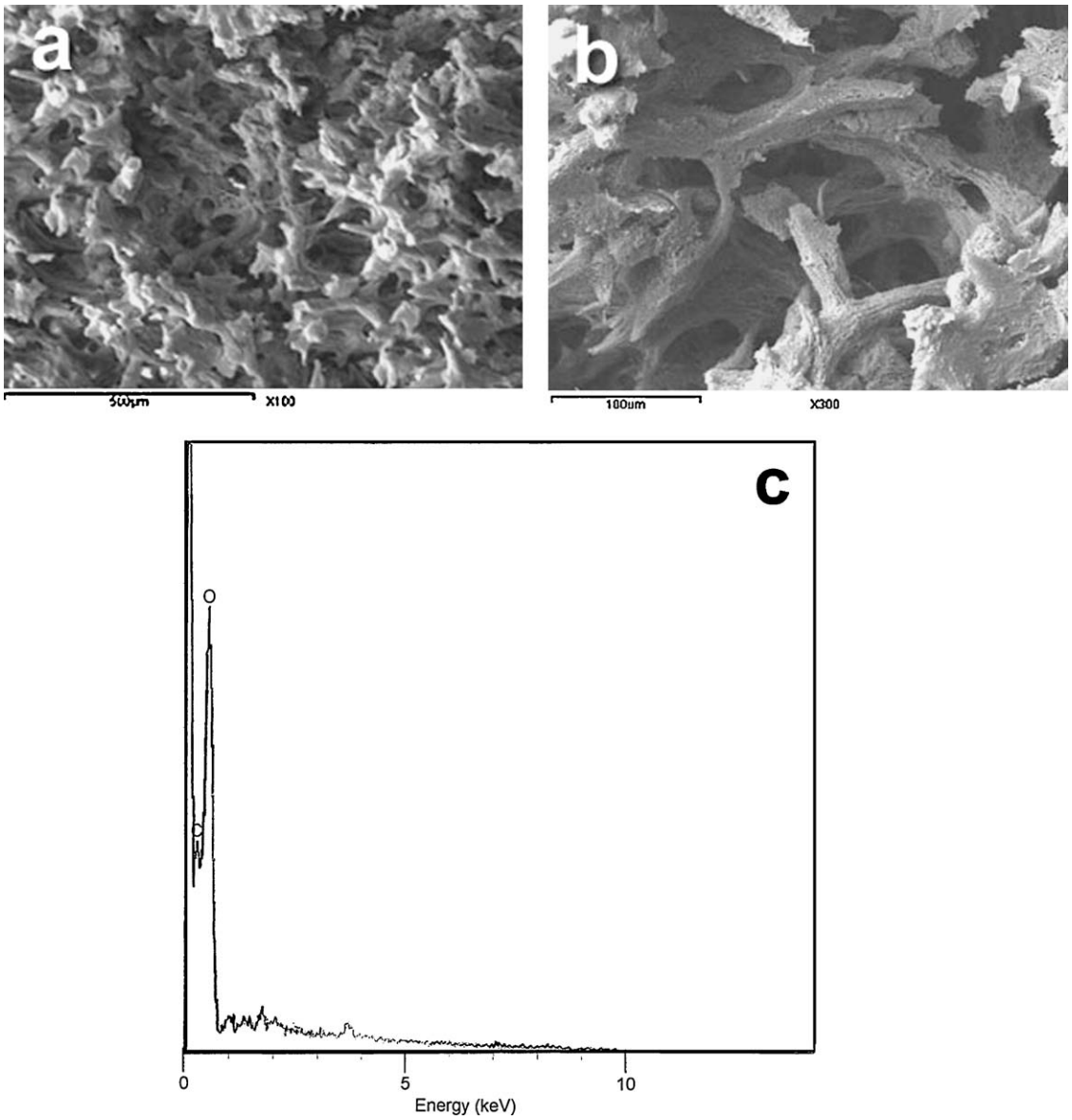

Fig. 2. SEM micrographs showing a cross-section of the neat polymer scaffold (PLA) at different magnifications (a and b). The figure also includes EDX analysis (c) of the PLA scaffold. The interconnected porous structure of the scaffold can be clearly noticed.

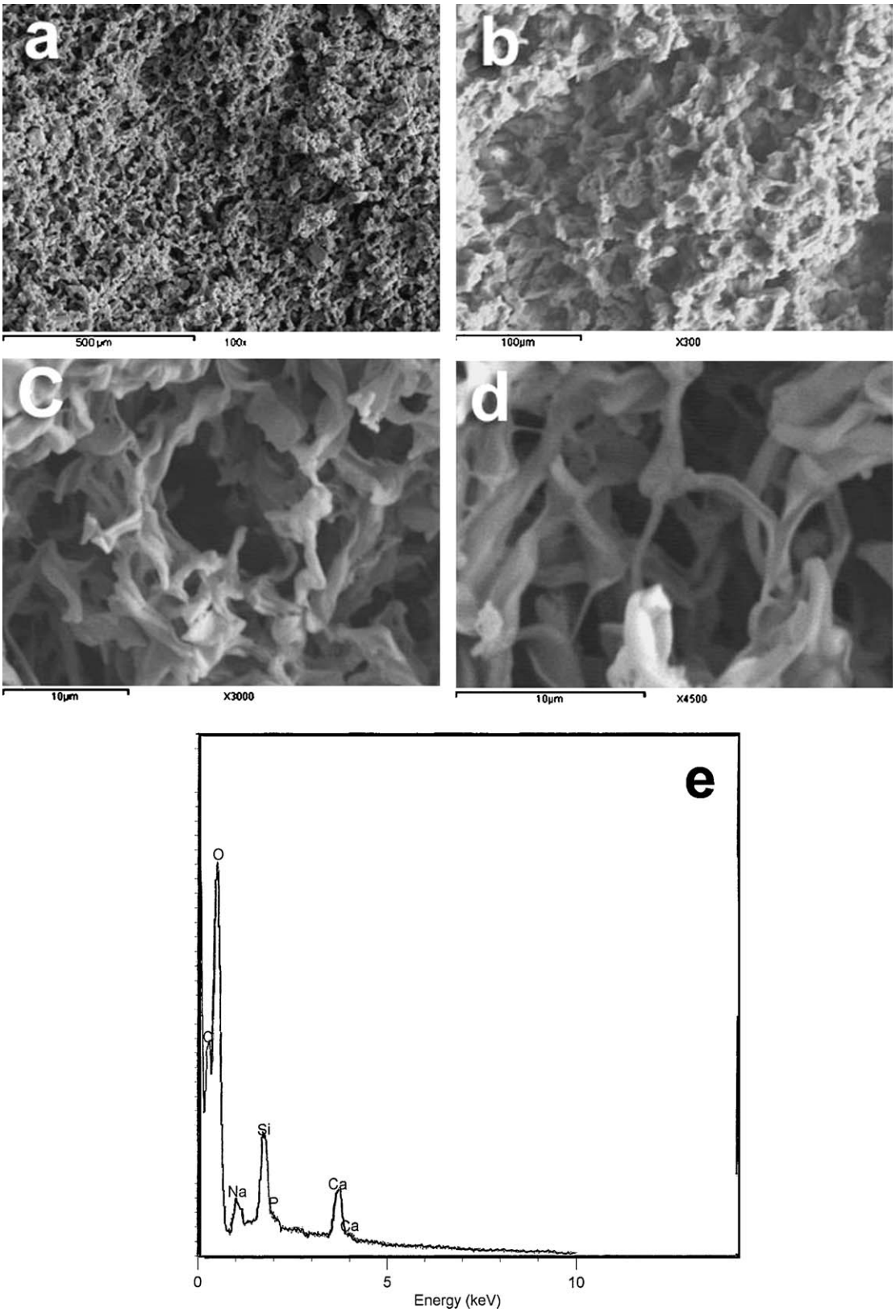

Fig. 3. SEM micrographs showing a cross-section of the SP25 (a–d) at different magnifications. The interconnected porous structure of the scaffolds can be clearly noticed. The figure also includes EDX analysis (e) of the SP25.

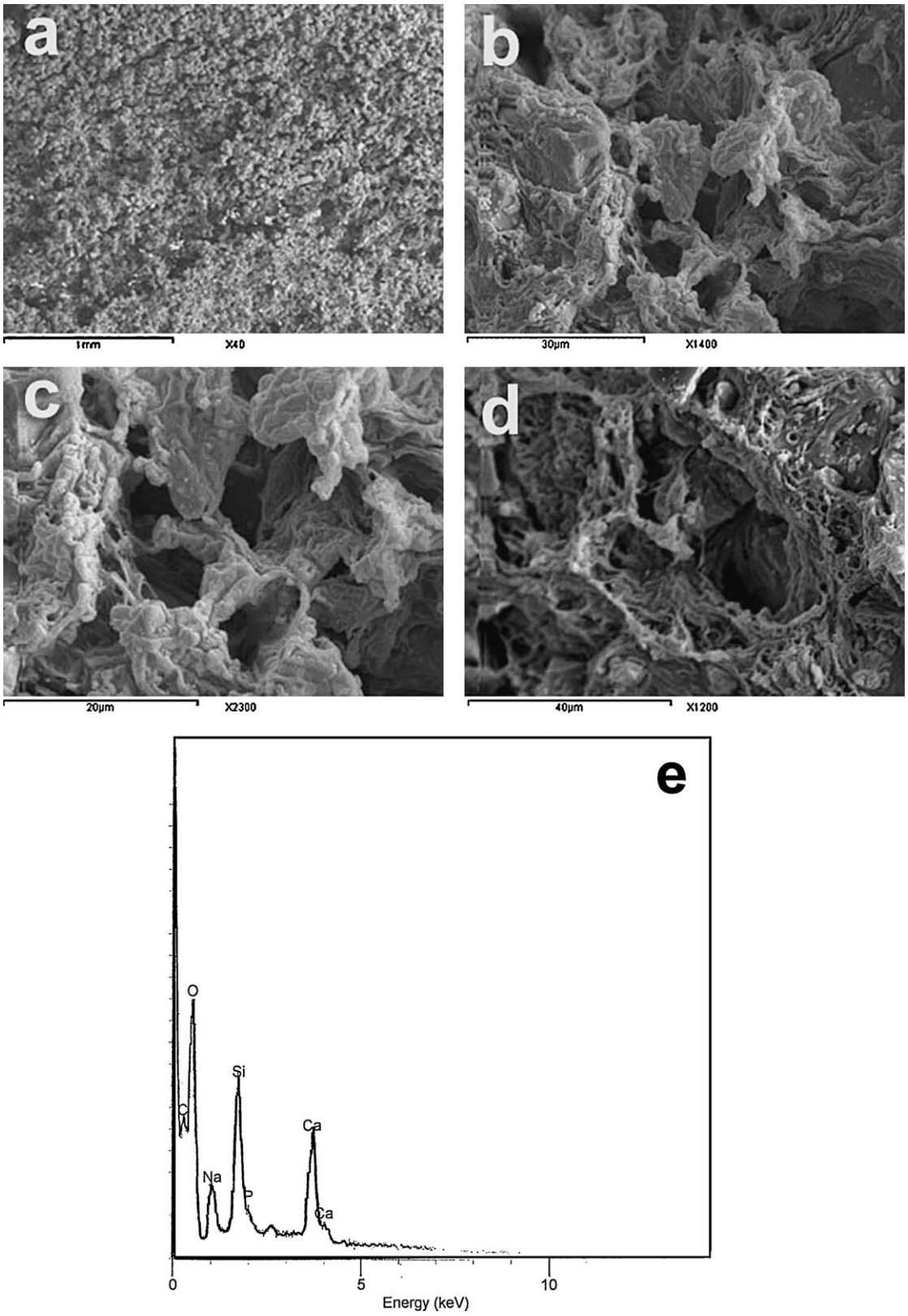

Fig. 4. SEM micrographs showing a cross-section of the SP50 (a–d) at different magnifications. The interconnected porous structure of the scaffolds can be clearly noticed. The figure also includes EDX analysis (e) of the SP50.

3. Results and discussions

3.1. Characterization

3.1.1. SEM examination

SEM micrographs of the silicate glass (S) is showed in Fig. 1(a and b). The figure includes its EDX analysis. SEM micrographs of a cross-section of the neat polymer scaffold (PLA) and composite scaffolds prepared by the freeze-extraction technique provided in Figs. 2–4. They also include their EDX analysis. For the PLA, a highly interconnected porous structure observed, with a maximum pore size of 200 μm (Fig. 2(a and b)). EDX analysis for the PLA showed only carbon and oxygen peaks (Fig. 2(c)). Examination of the SEM microphotographs of composite scaffolds revealed that their pore size decreased as their glass content increased. For the composite scaffold containing glass content up to 25 wt% (SP25), the maximum pore size decreased to 40 μm (see Fig. 3(a–d)). However, its porous structure remained interconnected with irregular pores. For SP50, the pore size further decreased as the glass content increased up to 50 wt%. It was 20 μm. Nevertheless, its porous structure interconnected with irregular pore morphology (see Fig. 4(a–d)). The presence of a glass filler in SP25 and SP50 confirmed by their EDX analysis as showed by Figs. 3(e) and 4(e), respectively. Their EDX spectra showed calcium, silica, phosphorous and sodium peaks, which were the main components of silicate-based bioactive glass (see Fig. 1(c)). In addition, it could be noticed that the intensity of these peaks increased as the glass contents increased from 25 wt% to 50 wt%.

In this study, the polymer solution froze at −80 °C, which was below the freezing point of the chloroform (−64 °C) [33], thus, inducing the solid–liquid phase separation by freezing the solvent. A continuous polymer rich phase formed by the aggregation of the polymer which expelled from every single solvent crystal. After removal of the solvent crystals by extraction, the interconnected porous structure of the polymer formed with pores similar to the geometry of the solvent crystals (see Fig. 2). The SEM micrographs demonstrated that the porosity of the polymer matrix could be affected by the incorporation of bioactive glass. When an inorganic filler, such as bioactive glass added to the polymer/solvent solution, the growth of solvent crystals impeded during the phase separation mechanism by the randomly distributed solid inorganic second phase, hence the porosity of the scaffold decreases and the pores became irregular in shape (see Figs. 3 and 4). Other studies reported the same conclusions [16,31]. The measurement of the porosity of the scaffolds by liquid displacement method [30,31] also confirmed those results (see Table 4).

3.1.2. Bulk density and apparent porosity

Table 4 illustrates the mean value of the bulk density and the apparent porosity measured by the liquid displacement method [30,31] for the neat polymer and composite scaffolds. The results indicated that the density increased with the increase of the bioactive glass content. On the contrary, the porosity decreased with increasing glass content. Other studies reported the same conclusions [16,31,34,23].

Table 4
The mean value of bulk density and apparent porosity measured by the liquid displacement method for the neat polymer and composite scaffolds.

Scaffold code	Apparent porosity (%)	Bulk density (g/cm^3)
PLA	56.56 ± 7.150	0.4169 ± 0.115
SP25	52.49 ± 5.643	0.4344 ± 0.114
SP50	48.74 ± 4.965	0.6658 ± 0.112

3.1.3. FTIR analysis

Fig. 5 shows the FTIR spectra of a neat polymer scaffold (PLA), composite scaffolds (SP25 and SP50) and silicate bioactive glass (S). For silicate bioactive glass (S), the spectrum showed the characteristic absorption bands of bioactive silicate glass reported by others [35,36]. Those bands were: [Si–O–Si] stretching at 1170 cm^{-1}, [Si–O–NBO] stretching at 963 cm^{-1}, [Si–O–Si] bending near 750 cm^{-1}, and PO_4 asymmetric bending at 575 cm^{-1}. For the neat polymer scaffold (PLA), the spectrum showed the typical characteristic absorption bands of poly(L-lactide) as reported elsewhere [37], which were carbonyl modes [C=O] at 1780 cm^{-1}, asymmetric CH_3 bending mode at 1464 cm^{-1}, symmetric CH_3 stretch at 1390 cm^{-1}, [C–O] stretching mode at 1147 cm^{-1} and other

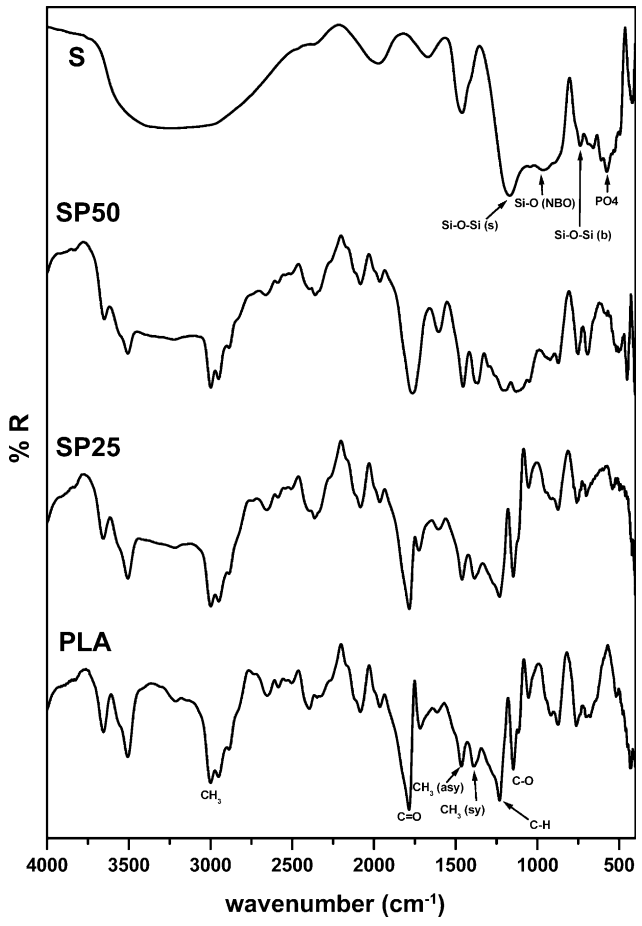

Fig. 5. FT-IR spectra of PLA, SP25, SP50 and S.

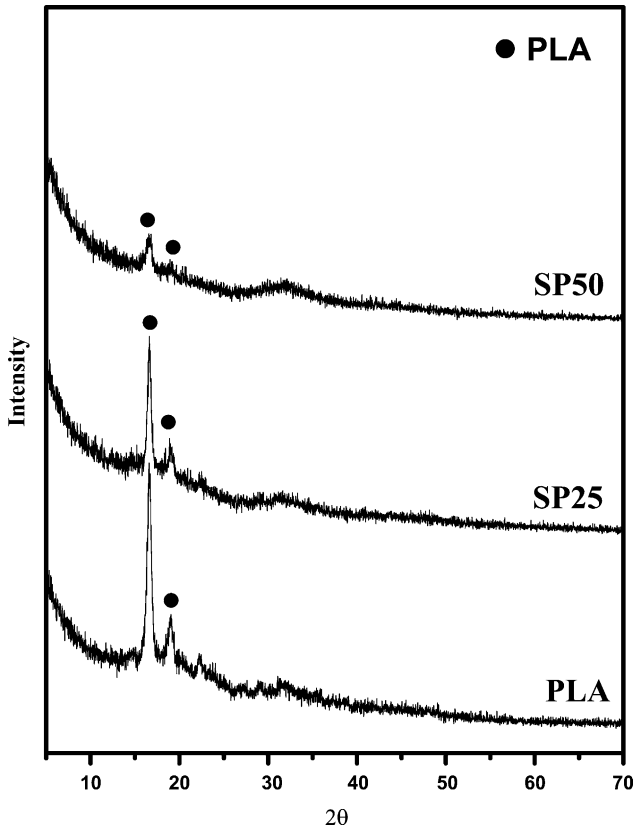

Fig. 6. XRD of SP25 and SP50 as compared with PLA.

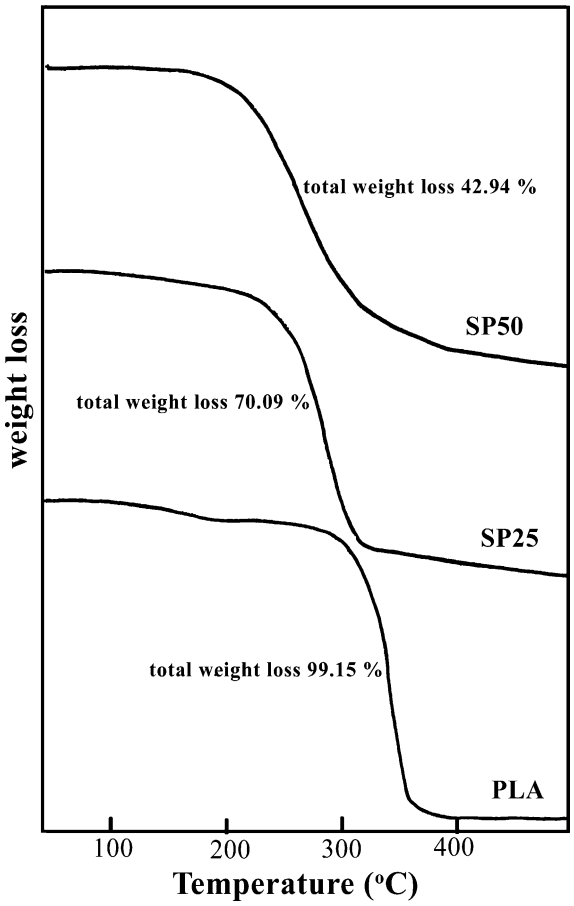

Fig. 7. Thermogravimetric analysis (TGA) of PLA, SP25 and SP50 scaffolds.

methyl bands at 3000 cm^{-1}. FTIR spectra of composite scaffolds (SP25 and SP50) contain all the characteristic absorption peaks of poly(L-lactide) and bioactive silicate glass. However, slight shift noticed for the main peaks of poly(L-lactide) to lower frequency, which might be attributed to some interaction between the polymer and the glass.

3.1.4. X-ray diffraction analysis (XRD)

Fig. 6 shows a comparison between the X-ray diffraction pattern of the neat polymer scaffold (PLA) and composite scaffolds. Two diffraction peaks located at $2\theta = 16.63$ and 18.86 saw in the X-ray diffraction pattern of the neat polymer scaffold and composite scaffolds corresponding to the crystal structure of the poly(L-lactide) [38]. However, we could observe from the figure that their intensity gradually decreased as the glass filler content increased in the composite scaffolds. That could be attributed to the interaction between the polymer and glass filler, and to the amorphous nature of glass filler, which had no definite crystalline peaks. Therefore, the two characteristic crystalline peaks of the poly(L-lactide) masked by the glass fillers.

3.1.5. Thermal analysis

The thermogravimetric analysis (TGA) of the neat polymer scaffold (PLA) and the composite scaffolds showed in Fig. 7. The TGA results of PLA showed that the thermal destruction of the polymer started at 300 °C and ended at 370 °C recording a total weight loss about 99.15% due to the release of organic materials. The thermal destruction of SP25 and SP50 occurred in the range of 220–310 °C and the total weight loss recorded for those composite scaffolds were 70.09% and 42.94% respectively due to release of organic materials. The glass content in the fabricated composite scaffolds could be calculated from the TGA data by subtracting the total weight loss that occurred for each composite scaffold, from the total weight loss that occurred for the neat polymer scaffold (PLA). Table 5 represents the glass content calculated from the TGA data and the total weight loss recorded for the scaffolds. The table also showed the calculated glass content according to Eq. (1) for comparison. The comparison showed a difference between the amount of the glass content calculated from TGA data and those calculated by Eq. (1). Such difference might be due to some partial sedimentation of the glass particles during scaffold fabrication [20].

Table 5
The glass content and the total weight loss recorded for the composite scaffolds.

Scaffold code	Total weight loss	Glass content calculated according TGA data	Glass content calculated according to Eq. (1)
PLA	99.15%	–	–
SP25	70.09%	29.06%	25%
SP50	42.94%	56.21%	50%

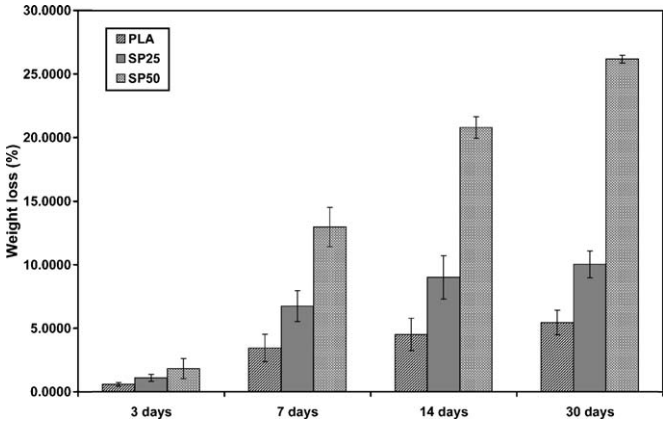

Fig. 8. The percentage of the weight loss of the SP25 and SP50 versus incubation time as compared to the PLA.

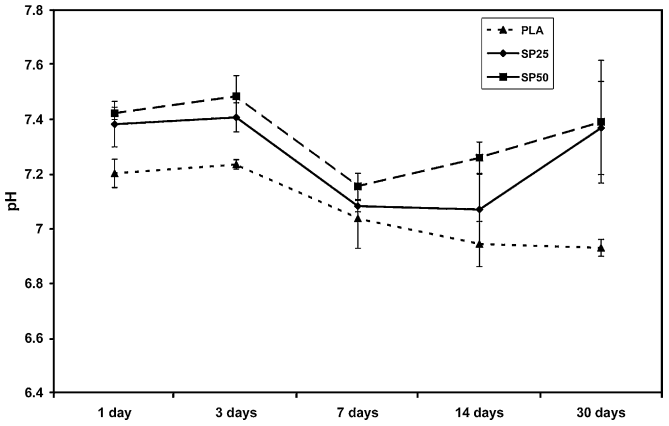

Fig. 10. pH values of PLA, SP25 and SP50 versus incubation time.

3.2. Degradation analysis

3.2.1. Evaluation of weight loss results

Fig. 8 shows the weight loss of the PLA, SP25 and SP50 versus incubation time. The weight loss of the PLA changed slightly during the whole incubation period as compared to that of SP25 and SP50, thus confirming the hydrophobic and slow degradation nature of the PLA. The figure also showed that there was a significant increase in the weight loss for both SP25 and SP50 as compared to the PLA at all time periods. In addition, the weight loss for the composite scaffolds containing silicate bioactive glass, increased with the increase of both immersion time and glass content. At the end of incubation time the weight loss was around 5.44%, 9.31% and 26.17% for the PLA, SP25 and SP50, respectively. The results indicated that the degradation rate of the scaffold enhanced by the presence of the hydrophilic fillers, such as silicate bioactive glass.

3.2.2. Explanation of the weight loss results

Bone engineering scaffold should had the advantage of degrading biologically with time with new tissue growth, so that it avoided the need for further surgery. Poly(L-lactide) polymers had good mechanical properties and could potentially be applied in load-bearing situations [6]. However, they had slow degradation rate. The results of the degradation studies in PBS indicated the possibility to modulate the degradation rate of the composite scaffolds by varying the glass content in order

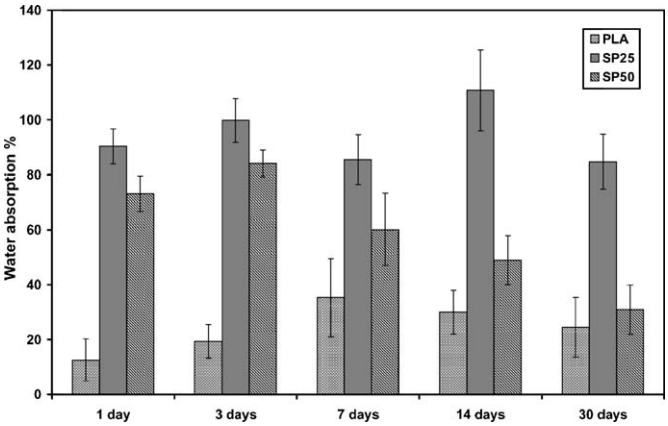

Fig. 9. The percentage of water absorption of the SP25 and SP50 versus incubation time as compared to with PLA.

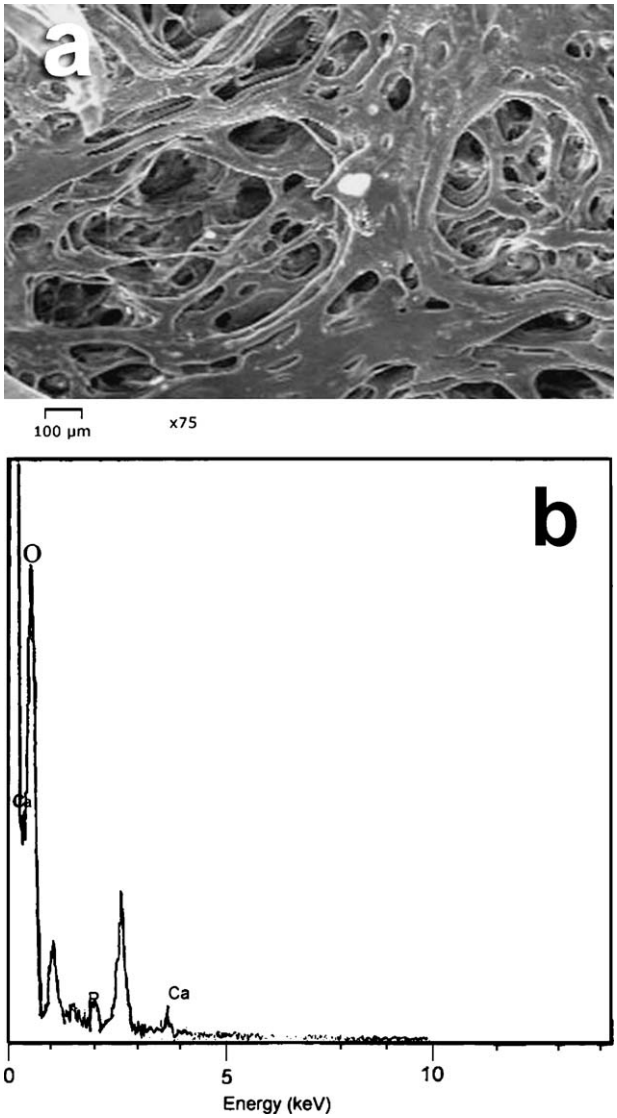

Fig. 11. SEM micrographs (a) and EDX analysis (b) of the surface of the neat polymer scaffold (PLA) and after immersion in the SBF for 30 days.

to reach to the optimal degradation rate suitable for bone engineering. The presented degradation results showed that the introduction of bioactive glasses to the polymer scaffolds resulted in an increased weight loss at all time periods. This increased weight loss might mainly be the result of glass particles dissolution. The results revealed also that the glass content influence the degradation rate of the composite scaffolds. Scaffolds with higher glass content had higher weight loss than those with lower glass content. This could be explained by the increased glass particles leaching out of the scaffolds containing higher glass content. From the obtained results, it was obvious that higher glass content resulted in faster degradation of the scaffold.

3.2.3. Evaluation and explanation of water absorption (WA) results

Fig. 9 shows the water uptake of PLA, SP25 and SP50 for different time periods. For PLA, the water uptake increased gradually and reached a maximum value at the end of the first week (35.28%), and then started to decrease gradually up to 24.39% at the end of the fourth week of incubation. The water uptake by the SP25 reached a maximum value (110.81%) at the end of the second week and then decreased to 84.71% at the end of the fourth week. In case of SP50, it exhibited a similar profile in the water absorption change to the PLA, but it reached the maximum value of 84.14% at the end of the third day of incubation, followed by a gradual decrease to reach its minimum value at the end of the fourth week (30.93%). Moreover, it could be observed from the same figure that SP25 and SP50 absorbed a significantly higher amount of water than PLA during the whole incubation time periods, which could be attributed to the hydrophobic nature of the PLA, as well as to the hydrophilic character of silicate bioactive glass. It has shown previously, that when silicate bioactive glass was subjected to hydrolysis, it forms SiOH groups on its surface [7]. Those groups could form hydrogen bonding with the water molecules, causing an increase in the water uptake by the scaffolds. Comparing the water uptake profile of SP25 and SP50, we observed that their ability to absorb water decreased with further increase in glass content over the whole incubation time periods. That was due to the decrease in porosity at higher filler contents (50 wt%), which agreed with the porosity

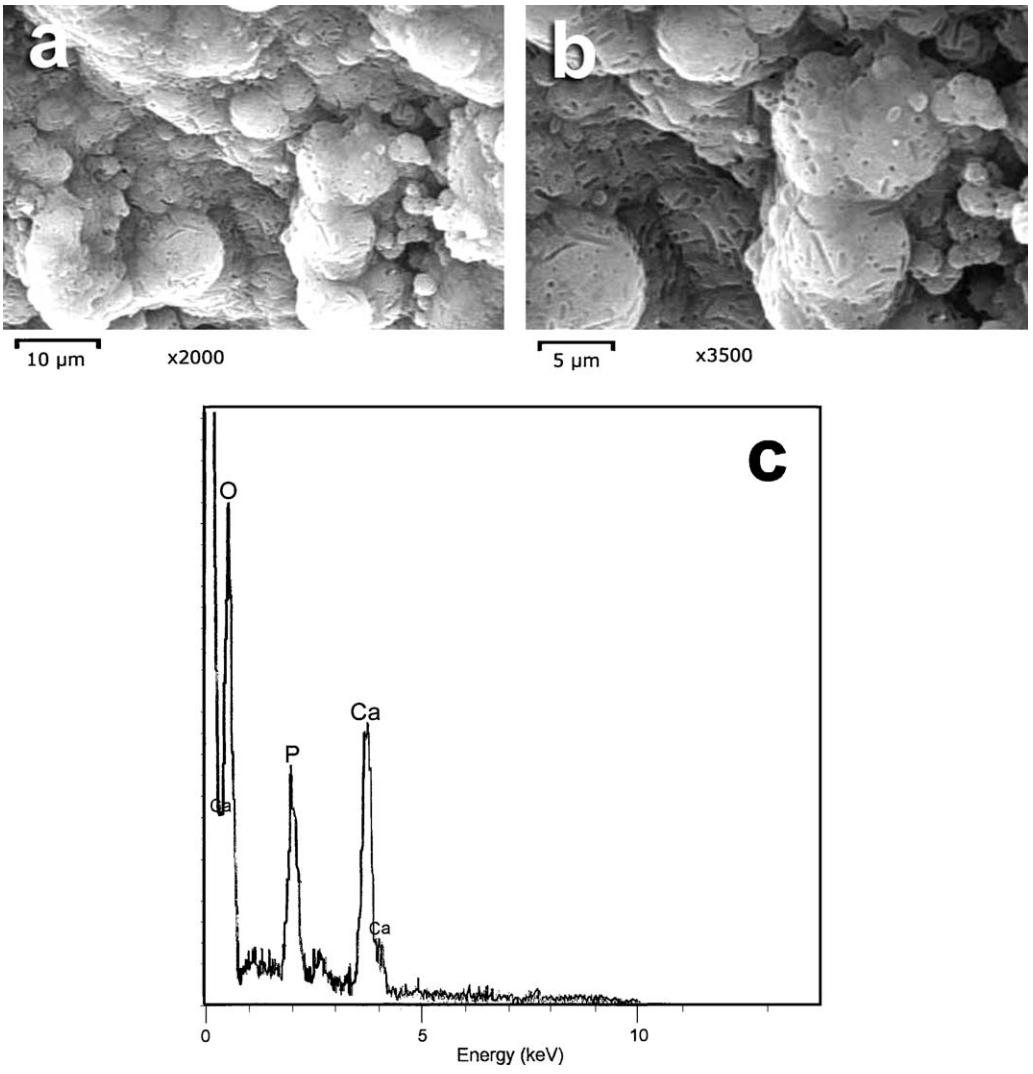

Fig. 12. SEM micrographs (a and b) and EDX analysis (c) of the surface of SP25 composite scaffold and after immersion in the SBF for 30 days.

measurement results showed in Table 3 and is consistent with previous findings by others [30,31].

3.2.4. Evaluation and explanation of pH measurements of incubation medium

The pH variation patterns of the phosphate buffer solution (PBS) containing PLA, SP25 and SP50, showed in Fig. 10. The pH of the incubation medium containing the PLA decreased from the initial value (7.4) to (7.2) at the first. After that it continued to decrease throughout the whole degradation period, and finally reached the value of 6.93 at the end of the incubation period (30 days). On the contrary, the pH of the incubation medium slightly increased to the value of 7.42 in the case of the SP50, and remained very close to the initial value in the case of SP25 (7.38) at the first day. Then it continued to increase to reach the values of 7.4 and 7.5 for SP25 and SP50 respectively

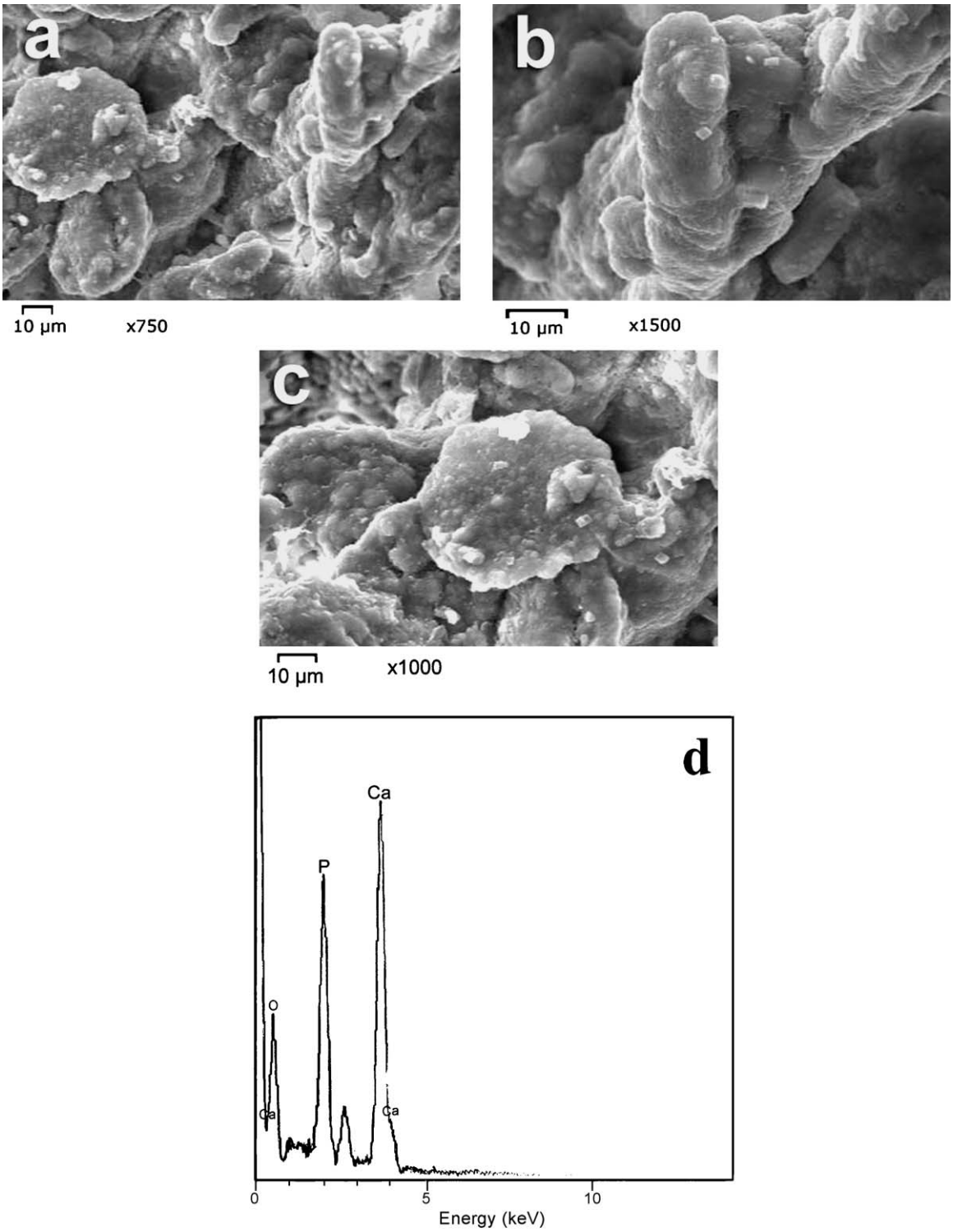

Fig. 13. SEM micrographs (a–c) and EDX analysis (d) of the surface of SP50 composite scaffold and after immersion in the SBF for 30 days.

at the third day of incubation. Finally, it reached the value of 7.37 and 7.39 for SP25 and SP50 respectively at the end of incubation period (30 days), which was significantly higher than the pH of the medium containing the PLA (6.95) at the end of incubation period. The results revealed that the silicate bioactive glass could neutralize the acidic degradation products of the polymer matrix.

It was important to realize that the acidic groups resulting from the degradation of the poly(L-lactide) results in pH decrease in the vicinity of the scaffold, which might be responsible for biocompatibility concerns emerged about its used for biomedical applications [39,40,41]. On the other hand, the dissolution of the silicate glass particles turned the medium alkaline due to their dissolution by-products. Therefore, the pH of the medium depends on both the degradation rate of the polymer matrix and the dissolution profile of the glass particles. Hence, one of the most important goals of the pH measurements, carried out that in this work, was to evaluate the ability of the bioactive glass fillers for compensating the acidic degradation products of the PLA scaffold. Boccaccini et al. [42] reported that the dissolution of alkaline ions from the bioactive glass particles locally compensate the acidification of the PBS due to acidic products of the polymer degradation. Silicate bioactive glasses release both calcium and sodium ions during their dissolution. Such ions locally compensate for the acidification of the medium due to acidic products of the polymer degradation. That buffering effect of the silicate bioactive glass previously reported elsewhere [43], and it has been considered to be an advantage for using bioactive glass particles as a filler in composite scaffold to avoid possible inflammatory response, due to acidic degradation of the polymer. This behavior might be due to the fact that the acidic and basic degradation products of the polymer and glass respectively could be neutralized and resulting in maintaining the medium at a physiological pH [43,44].

3.3. In vitro bioactivity evaluation

3.3.1. Scanning electron microscope coupled with energy-dispersive X-ray spectroscopy (SEM/EDX)

Fig. 11(a) shows the SEM micrograph of the surface morphology of the neat polymer scaffolds (PLA) immersed in SBF for 30 days. The figure clearly showed that there was no formation of the hydroxyapatite layer on its surface. EDX analysis of its surface confirmed those results (see Fig. 11(b)), which showed that the main elements were carbon and oxygen, with only a negligible amounts of calcium and phosphorous. On the other hand, examining the SEM micrographs of the surface of the scaffold containing glass content up to 25 wt% (SP25) (Fig. 12(a and b)), showed that it completely covered with a thick layer of a spherical crystals of porous structure. EDX analysis (Fig. 12(c)) showed that the chemical composition of that spherical layer could be assigned to calcium-deficient and non-stoichiometric apatite with Ca/P ratio of 1.49. Furthermore, the SEM micrographs of the scaffold containing glass content up to 50 wt% (SP50), showed that the surface fully covered with a thick layer composed of both spherical and rod like crystals (Fig. 13(a–c)). The EDX analysis (Fig. 13(d)) revealed that this layer composed of calcium-deficient and non-stoichiometric apatite with Ca/P ratio of 1.62. Comparing the EDX analyses for both SP25 and SP50, showed that the apatite layer formed on the surface of SP50 was more mineralized than that formed on the surface of SP25. Examination of the SEM micrographs for PLA, SP25 and SP50 clearly indicated that the addition of silicate bioactive glass to the scaffolds induced the bioactive properties to them, which could improve their bone bonding ability in vivo. The formation of the hydroxyapatite layer on the surface of composite scaffolds (SP25&SP50), could be explained by the hydrolysis of ester bonds of the polymer, and the formation of carboxylate groups (COOH). Those functional groups had the ability to attract silica ions, released from the scaffolds, due to the dissolution of the glass particles. In turn those ions act as nucleation sites for both calcium and phosphorus ions, leading to the formation of hydroxyapatite layer on the surfaces of the composite scaffolds [45,46].

3.3.2. Thin film X-ray diffraction analysis (TF-XRD)

The TF-XRD patterns of the surface of the neat polymer scaffold (PLA) and composite scaffolds before and after immersion in the SBF for different time periods showed in Figs. 14–16. Examination of TF-XRD patterns of the neat polymer scaffold showed no sign of apatite formation even after 4 weeks, and only the typical crystalline diffraction pattern of

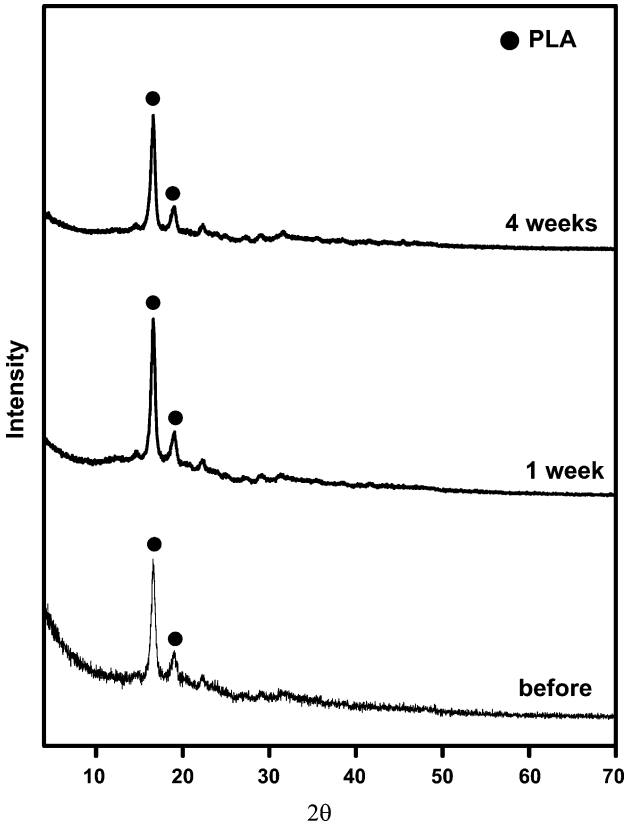

Fig. 14. Thin film X-ray of PLA, before and after immersion in SBF for 30 days.

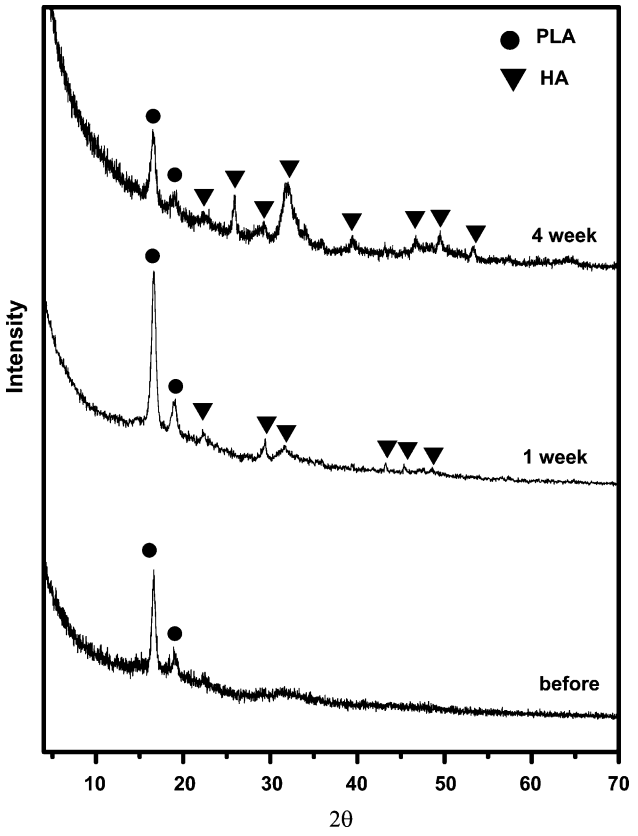

Fig. 15. Thin film X-ray of SP25, before and after immersion in SBF for 30 days.

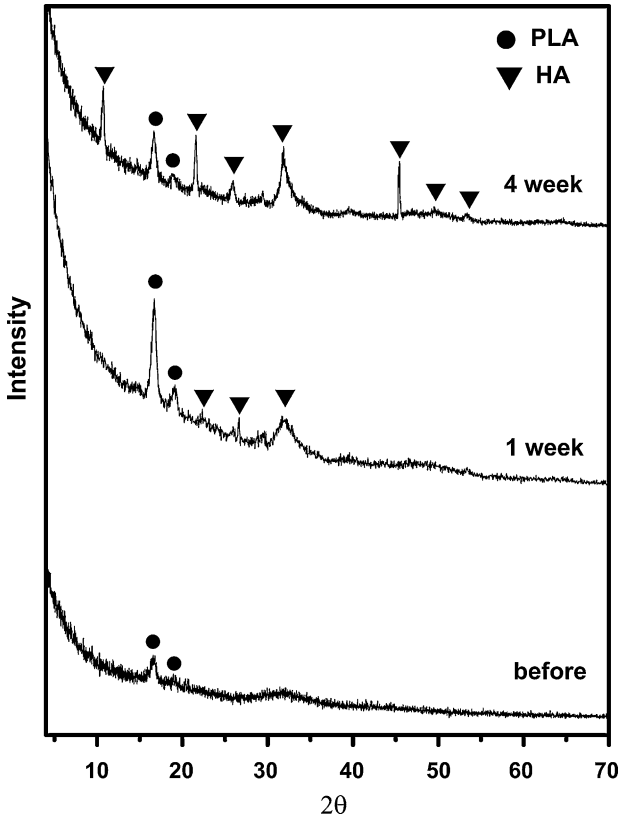

Fig. 16. Thin film X-ray of SP50, before and after immersion in SBF for 30 days.

the polymer observed [38]. Two sharp XRD peaks of the crystalline poly(L-lactide) found at 2θ values of 16.63 and 18.86 corresponding to d-spacings of 5.34 Å and 4.67 Å respectively (Fig. 14). On the other hand, for the composite scaffolds, the figures clearly indicate the formation of the apatite layer, on the surfaces of the SP25 and SP50, after 1-week immersion in the SBF. The typical diffraction pattern of the crystalline apatite could be observed, which was associated with an evident peaks at d-spacing values of 2.81 Å, 2.72 Å and 2.77 Å [matched with the corresponding ICSD card no (016-742)]. Those diffraction peaks became sharper and their intensity increased as the incubation time increased to 4 weeks, indicating a higher apatite crystallinity. In addition, the appearance of other less intense peaks at d-spacing values of 2.49 Å, 2.28 Å, 1.94 Å, 1.84 Å and 1.72 Å [matched with the corresponding ICSD card no (016-742)] was also noticed from diffraction patterns of the SP25 and SP50, after 4 weeks of incubation in SBF (Figs. 15 and 16). Those results further confirmed the apatite formation and crystallization. The diffraction peak of the formed apatite at d-spacing value of 8.27 Å appeared only for SP50 sample [matched with ICSD card no (016-742)], indicating the complete crystallization of the apatite layer (Fig. 16). From the thin-film X-ray diffraction analysis (TF-XRD), it obviously deduced that the addition of the glass to the polymer matrix induced the apatite formation and improved their bioactive behaviors. It also revealed that the apatite layer formed after 1 week of immersion in the SBF indicating a high rate of bioactivity.

4. Conclusion

- The freeze-extraction technique used successfully in the fabrication of silicate glass/poly(L-lactide) composite scaffolds. The neat polymer scaffold (PLA) showed a highly interconnected porous structure and average pore size (few microns to 200 μm). Increasing the glass content to 25 wt% (SP25 sample) and to 50 wt% (SP50 sample) resulted in a decrease of their pore size. Nevertheless, their porous structure was interconnected.
- The degradation results showed that the introduction of bioactive glasses to the polymer scaffolds resulted in an increased weight loss at all time periods. In addition, SP25 and SP50 absorbed a significantly higher amount of water than the PLA over the whole time period, which could be attributed to the hydrophobic nature of the PLA as well as to the hydrophilic character of the silicate bioactive glass.
- Silicate bioactive glass used as a filler in composite scaffolds could compensate the released acidity during the degradation of the polymer. That buffering effect of glass might provide a new method to avoid the possible inflammation resulted from the acidic degradation products of the polyesters.
- The results obtained from this study indicate the possibility to modulate the degradation rate of the composite scaffolds by varying their glass content.
- The addition of silicate bioactive glass to the scaffolds induced the bioactive properties to them, which could improve their bone bonding ability in vivo.

References

[1] M. Braddock, P. Houston, C. Campbell, P. Ashcroft, Born again bone: Tissue engineering for bone repair, News Physiol. Sci. 16 (2001) 208–213.

[2] E.L. Chaikof, H. Matthew, J. Kohn, A.G. Mikos, G.D. Prestwich, C.M. Yip, Biomaterials and scaffolds in reparative medicine, Ann. NY Acad. Sci. 961 (2002) 96–105.

[3] S. Levenberg, R. Langer, Advances in Tissue Engineering Current Topics in Developmental Biology, vol. 61, Academic Press, New York, 2004, pp. 113–134.

[4] L.G. Griffith, Emerging design principles in biomaterials and scaffolds for tissue engineering, Ann. NY Acad. Sci. 961 (2002) 83–95.

[5] V. Karageorgiou, D. Kaplan, Porosity of 3D biomaterial scaffolds and osteogenesis, Biomaterials 26 (2005) 5474–5491.

[6] J. Jagur-Grodzinski, Biomedical application of functional polymers, Reactive Funct Polym 39 (1999) 99–138.

[7] L.L. Hench, J. Wilson (Eds.), An Introduction to Bioceramics, 2nd edition, Word Scientific, London, 1999.

[8] L.L. Hench, Bioceramics, J. Am. Ceram. Soc. 81 (1998) 170.

[9] I.D. Xynos, A.J. Edgar, L.D.K. Buttery, L.L. Hench, J.M. Polak, Ionic products of bioactive glass dissolution increase proliferation of human osteoblasts and induce insulin-like growth factor II mRNA expression and protein synthesis, Biochem. Biophys. Res. Commun. 276 (2000) 461–465.

[10] O. Tsigkou, J.R. Jones, J.M. Polak, M.M. Stevens, Differentiation of fetal osteoblasts and formation of mineralized bone nodules by 45S5 Bioglass® conditioned medium in the absence of osteogenic supplements, Biomaterials 30 (21) (2009) 3542–3550.

[11] L. Larry, Hench Genetic design of bioactive glass, J. Eur. Ceram. Soc. 29 (April (7)) (2009) 1257–1265.

[12] I.D. Xynos, A.J. Edgar, L.D.K. Buttery, L.L. Hench, M. Polak, Gene expression profiling of human osteoblasts following treatment with the ionic products of Bioglass 45S5 dissolution, J. Biomed. Mater. Res. 55 (2001) 151–157.

[13] H. Ohgushi, Y. Dohi, T. Yoshikawa, S. Tamai, S. Tabata, K. Okunaga, et al., Osteogenic differentiation of cultured marrow stromal stem cells on the surface of bioactive glass ceramics, J. Biomed. Mater. Res. 32 (1996) 341–348.

[14] L.L. Hench, R.J. Splinter, W.C. Allen, Bonding mechanisms at the interface of ceramic prosthetic materials, J. Biomed. Mater. Res. Symp. 2 (1971) 117–141.

[15] H. Oonishi, S. Kushitani, H. Iwaki, Comparative bone formation in several kinds of bioceramic granules, in: J. Wilson, L.L. Hench, D. Greenspan (Eds.), Eighth International Symposium on Ceramics in Medicine, Tokyo, Japan, (1995), pp. 137–144.

[16] V. Maquet, A.R. Boccaccini, L. Pravata, I. Notingher, R. Jerome, Porous poly([alpha]- hydroxyacid)/Bioglass(R) composite scaffolds for bone tissue engineering. I. Preparation and in vitro characterization, Biomaterials 25 (2004) 4185–4194.

[17] J.A. Roether, A.R. Boccaccini, L.L. Hench, V. Maquet, S. Gautier, R. JérÔme, Development and in vitro characterization of novel bioresorbable and bioactive composite materials based on polylactide foams and Bioglass® for tissue engineering applications, Biomaterials 23 (2002) 3871–3878.

[18] S. Verrier, J.J. Blaker, V. Maquet, L.L. Hench, A.R. Boccaccini, PDLLA/Bioglass® composites for soft-tissue and hard–tissue engineering: an in vitro cell biology assessment, Biomaterials 25 (2004) 3013–3021.

[19] J. Yao, S. Radin, P.S. Leboy, P. Ducheyne, The effect of bioactive glass content on synthesis and bioactivity of composite poly (lactic-co-glycolic acid)/bioactive glass substrate for tissue engineering, Biomaterials 26 (2005) 1935–1943.

[20] J.J. Blaker, V. Maquet, R. Jérôme, A.R. Boccaccini, S.N. Nazhat, Mechanical properties of highly porous PDLLA/Bioglass_composite foams as scaffolds for bone tissue engineering, Acta Biomater. 1 (2005) 643–652.

[21] O. Tsigkou, L.L. Hench, A.R. Boccaccini, J.M. Polak, M.M. Stevens, Enhanced differentiation and mineralization of human fetal osteoblasts on PDLLA containing Bioglass® composite films in the absence of osteogenic supplements, J. Biomed. Mater. Res. 80A (2007) 837–851.

[22] T. Niemelä, H. Niiranen, M. Kellomäki, Self-reinforced composites of bioabsorbable polymer and bioactive glass with different bioactive glass contents. Part II. In vitro degradation, Acta Biomater. 4 (2008) 156–164.

[23] X. Li, J. Shi, X. Dong, L. Zhang, H. Zeng, A mesoporous bioactive glass/polycaprolactone composite scaffold and its bioactivity behavior, J. Biomed. Mater. Res. 84A (2008) 84–91.

[24] H.H. Lu, A. Tang, S.C. Oh, J.P. Spalazzi, K. Dionisio, Compositional effects on the formation of a calcium phosphate layer and the response of osteoblast-like cells on polymer-bioactive glass composites, Biomaterials 26 (2005) 6323–6334.

[25] H.W. Kim, H.H. Lee, G.S. Chun, Bioactivity and osteoblast responses of novel biomedical nanocomposites of bioactive glass nanofiber filled poly(lactic acid), J. Biomed. Mater. Res. 85A (2008) 651–663.

[26] A.R. Boccaccini, J.J. Blaker, V. Maquet, R.M. Day, R. Jérôme, Preparation and characterisation of poly(lactide-co-glycolide) (PLGA) and PLGA/Bioglass® composite tubular foam scaffolds for tissue engineering applications, Mater. Sci. Eng. C25 (2005) 23–31.

[27] S.G. Kazarian, K.L.A. Chan, V. Maquet, A.R. Boccaccini, Characterisation of bioactive and resorbable polylactide/Bioglass® composites by FTIR spectroscopic imaging, Biomaterials 25 (2004) 3931–3938.

[28] V. Maquet, A.R. Boccaccini, L. Pravata, I. Notingher, R. Jérôme, Preparation, characterization, and in vitro degradation of bioresorbable and bioactive composites based on Bioglass®-filled polylactide foams, J. Biomed. Mater. Res. A 66A (2003) 335–346.

[29] M.H Ho, P.Y. Kuo, H.J. Hsieh, T.Y. Hsien, L.T. Hou, J.Y. Lai, D.M. Wang, Preparation of porous scaffolds by using freeze-extraction and freeze-gelation methods, Biomaterials 25 (2004) 129–138.

[30] J. He, D. Li, Y. Liu, B. Yao, B. Lu, Q. Lian, Fabrication and characterization of chitosan/gelatin porous scaffolds with predefined internal microstructures, Polymer 48 (2007) 4578–4588.

[31] R. Zhang, P.X. Ma, Poly(a-hydroxyl acids)/hydroxyapatite porous composites for bone-tissue engineering, I. Preparation and morphology, J. Biomed. Mater. Res. 44 (1999) 446–455.

[32] T. Kokubo, H.M. Kim, M. Kawashita, H. Takadama, T. Miyazaki, M. Uchida, T. Nakamure, Nucleation and growth of apatite on amorphous phases in simulated body fluid, Glastech. Ber. Glass Sci. Technol. 73 (2001) 247–254.

[33] A. Smith, P.E. Heckelman, M.J. ONeil, S. Budavari, Merck Index: An Encyclopedia of Chemicals, Drugs and Biologicals, 13th edition, John Wiley& Sons, New York, 2001.

[34] Y.Y. Hsu, J.D. Gresser, D.J. Trantolo, C.M. Lyons, P.R. Gangadharam, D.L. Wise, Effect of polymer foam morphology and density on kinetics of in vitro controlled release of isoniazid from compressed foam matrices, J. Biomed. Mater. Res. 35 (1) (1997) 107–116.

[35] C.Y. Kim, A.E. Clark, L.L. Hench, Early stages of calcium phosphate layer formation in bioglasses, J. Non-Cryst. Solids 113 (1989) 195–202.

[36] C.Y. Kim, A.E. Clark, L.L. Hench, J. Biomed. Mater. Res. 26 (1992) 1147.

[37] P. Anurag, C.P. Girish, B.A. Pranesh, Synthesis of polylactic acid–polyglycolic acid blends using microwave radiation, J. Mech. Behav. Biomater. (1) (2008) 227–233.

[38] Z. Zhou, J. Ruan, J. Zou, Bioactivity of bioresorbable composite based on bioactive glass and poly-L-lactide, Trans. Nonferrous Met. Soc. China 17 (2007) 399–494.

[39] A.R. Boccaccini, V. Maquet, Bioresorbable and bioactive polymer/Bioglass® composites with tailored pore structure for tissue engineering applications, Compos. Sci. Technol. 63 (2003) 2417–2429.

[40] C. Martin, H. Winet, J.Y. Bao, Acidity near eroding polylactidepolyglycolide in vitro and in vivo in rabbit tibial bone chambers, Biomaterials 17 (1996) 2373–2380.

[41] W. Heidemann, S. Jeschkeit-Schubbert, K. Ruffieux, J.H. Fischer, H. Jung, G. Krueger, et al., pH-stabilization of predegraded PDLLA by an admixture of water-soluable sodiumhydrogenphosphate-results of an in vitro- and in vivo-study, Biomaterials 23 (2002) 3567–3574.

[42] A.R. Boccaccini, J.A. Roether, L.L. Hench, V. Maquet, R. Jérôme, A composites approach to tissue engineering, Ceram. Eng. Sci. Proc. 23 (2002) 805–816.

[43] H.Y. Li, J. Chang, pH-compensation effect of bioactive inorganic fillers on the degradation of PLGA, Compos. Sci. Technol. 65 (2005) 2226–2232.
[44] A. Stamboulis, L.L. Hench, A.R. Boccaccini, J. Mater. Sci. Mater. Med. 13 (2002) 843–848.
[45] K. James, H. Levene, J. Parsons, J. Kohn, Small changes in polymer chemistry have a large effect on the bone–implant interface: evaluation of a series of degradable tyrosinederived polycarbonates in bone defects, Biomaterials 20 (1999) 2203–2212.
[46] T. Jaakkola, J. Rich, T. Tirri, T.N. Arhi, M. Jokinen, J. Seppälä, A. Yli-Urpo, In vitro Ca-P precipitation on biodegradable thermoplastic composite of poly(ecaprolactone-codl-lactide) and bioactive glass (S53P4), Biomaterials 25 (2004) 575–581.